Proceedings of the 12th IEEE International
Conference on Nano/Micro Engineered and Molecular Systems
April 9-12, 2017, Los Angeles, USA

Optical Propagation of Blue LED Light in Brain Tissue and Parylene-C

Tian Xie, Xiaopeng Bi, Rui Luo, Fan Bin, Zhe Wang, Wen Li*
Electrical and Computer Engineering, Michigan State University, East Lansing, MI 48824
*E-mail: xietian1@msu.edu

***Abstract*- Understanding the propagation of LED light in the brain tissue can facilitate the advanced development of LED-based neuroprosthetic devices for optogenetic applications. In this work, the attenuation coefficient of blue LED light in thin tissue slices and Parylene-C films were quantified, which is 19.9 cm^{-1} and 1.70 cm^{-1}, respectively. Optical simulations in TracePro show good agreement with the experiments.**

Keywords— Micro-light-emitting diode; optical propagation; light attenuation coefficient.

I. Introduction

As a revolutionary neuromodulation technology, optogenetics offers remote manipulation on neural activities of genetically-targeted neural cells with millisecond temporal precision through light illumination [1-7]. Compared to electrical stimulation, optogenetics has unique benefits including specificity control of neural cell types as well as minimal artifacts and instrumental interferences with electrophysiological recording [8,9]. Application of optogenetics in neuroscience studies has created an increasing need for the development of light sources and the instruments for light delivery. Among various light sources, micro-light-emitting diodes (μ-LEDs) are favored for its high power efficiency, low cost, and capability of complex system integration [10-16]. Successful *in-vivo* optogenetic stimulation on neural cells with the employment of μ-LEDs has been widely reported [17-21].

Unlike lasers and laser diodes, μ-LEDs usually emit uncollimated light beams with wide irradiation angles, which increases light absorption and scattering while transmitting in a medium. However, there is little available information on the propagation of LED light in brain tissues and materials commonly used in neuroprosthetic device packaging. Lack of such information limits further development on light delivery systems for optogenetics.

In this work, we explored an attenuation coefficient to quantify the propagation of LED light through different materials. The attenuation coefficient of rat cortical tissue and Parylene-C film has been successfully obtained by a linear fitting on a series of measured light attenuation ratio and the corresponding thicknesses.

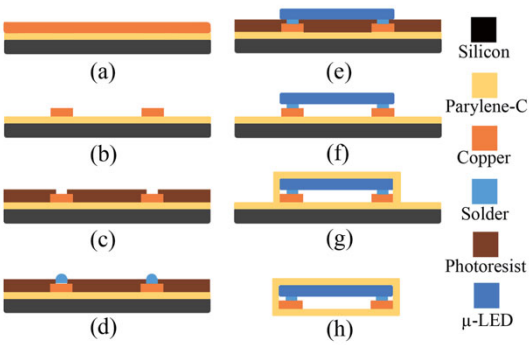

Fig.1 Schematic illustration of the process flow of μ-LED neural stimulators on Parylene-C substrates. (a) Parylene-C and copper deposition; (b) copper patterning; (c) photoresist coating and patterning; (d) applying low melting point (LMP) solder; (e) μ-LED assembly; (f) photoresist removal; (g) Parylene-C deposition; (h) peeling μ-LED stimulators off silicon substrates.

II. Fabrication

The LED light source used for the experiment was fabricated by flip chip bonding μ-LEDs (Cree® TR2227TM, 470nm wavelength, 220 μm × 270 μm ×50 μm) on copper pads that were pre-patterned on either polyimide (DupontTM Pyralux® AP7163E) or Parylene-C substrates. Wires were attached to the leads using silver paste and encapsulated by epoxy. In order for better protection, the light sources were subsequently coated with a 10-μm-thick Parylene-C film through vacuum chemical vapor deposition (CVD) using a PDS 2010 Labcoter® 2 (Specialty Coating Systems). The detailed process flow of such μ-LED neural stimulators on Parylene-C substrates is schematically illustrated in Fig. 1. To avoid overheating of μ-LEDs, low melting point (LMP, Alloy Field's Metal) solder was applied onto the pads in a diluted hydrogen chloride solution (pH=1) and the soldering process was carried out at 100 °C on a hot plate. Optical images of a fabricated μ-LED neural stimulator is shown in Fig. 2.

III. Method

When light travels through a medium with thickness t and attenuation coefficient α, the exponential decay of light can

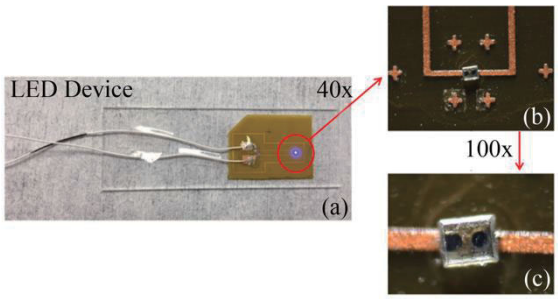

Fig. 2 (a) A fabricated μ-LED neural stimulator with light illumination. (b) Microscopic image of the assembled μ-LED chip at 40x magnification. (c) Microscopic image of the assembled μ-LED chip at 100x magnification.

be calculated using the following equation:

$$I = I_0 \times e^{-\alpha t} \quad (1)$$

where I_0 and I are the intensity of incoming light and output light, respectively. In this study, I_0 and I through different materials were first measured using a photodetector (Model 815 Series, Newport, Inc). Then a linear fitting was performed on a series of the logarithm of I_0/I as a function of the corresponding thicknesses t. The obtained slope of linear curves is equivalent to the attenuation coefficient of a specific medium.

Two types of samples were explored: 1) brain tissue slices with a thickness range of 100-300 μm, and 2) Parylene-C films with a thickness range of 15-100 μm. The brain tissue slices were collected from a rat that was perfused transcardially with 0.5L of 0.9% saline followed by 1.0L of a 10% formalin solution. Parylene-C is known as an optically transparent polymer coating material, which has many prominent advantages such as high chemical and biological stability, hydrolysis resistance, non-toxic and most importantly, biocompatibility. Parylene-C is selected in this study because it has been widely used in the construction of neural implant devices. During the experiments, the thickness of the tissues slices was estimated by measuring the difference in microscope focusing distance between the top and bottom surfaces of the tissue slices. The thicknesses of the Parylene were measured using a profilometer. The recorded thicknesses were used for drawing and analyzing the relationship between attenuation ratio and the thickness of rat brain tissue slices or Parylene-C films.

Fig. 3(a) shows the measurement setup where the sample film was carefully aligned and sandwiched between the assembled μ-LED chip and the photodetector. The photodetector was fixed in a 3-D printed holder to maintain a constant distance from the sample. The μ-LED was driven by 2.6 V to enable stable illumination. Fig. 3(b) schematically illustrates the setup of the measurement. It is noteworthy that the glass slide was covered by a black tape with an opening in the middle, which blocked the unconsidered light beam and only allowed the light passing through the rat brain cortical tissue to be collected by the photodetector.

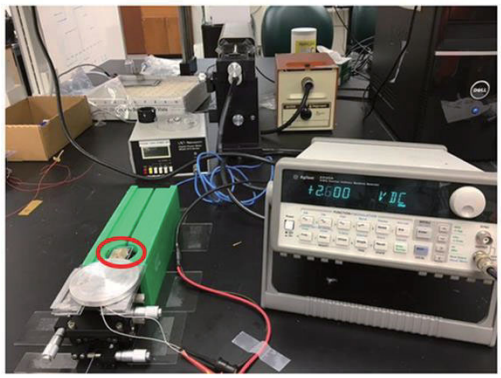

(a)

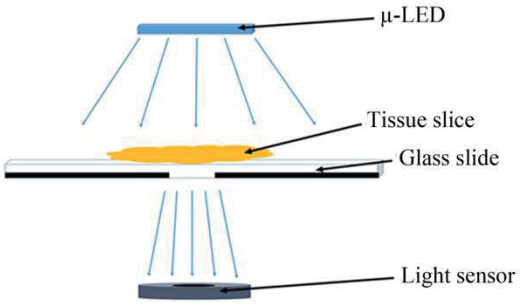

(b)

Fig. 3. (a) Experimental setup for measuring the light attenuation through different materials. (b) Schematic illustration of the measurement setup (the part circled in (a)), where the tissue slice was placed on a glass slide and sandwiched between the assembled μ-LED chip and the photodetector.

IV. Result and Discussions

A. Attenuation coefficient of brain tissue slices with different time durations for exposure

It is found that, as time passes by, the tissues exposed in air dry out gradually due to evaporation, which is likely to cause uncertainty to light attenuation. In order to minimize the influence of the tissue wetness on the light attenuation measurement, the tissue slices that were exposed in air for either 10 mins or 30 mins were firstly studied. To eliminate the influence caused by temperature and humidity, the experiments on both groups of the brain tissues were conducted under the same room temperature and same humidity.

After being exposed to air for 30 mins, the color of the brain tissues changed from transparent to a milky color. Consequently, as the thickness of the samples increases, the attenuation coefficient increases more significantly than the 10-min-dry sample, as shown in Fig. 4. When the thickness of the brain tissue slices increases to a certain degree, the attenuation of LED light will become much higher than 10-min-sample. As a result, after a long time of exposure to air, the brain tissue slices metamorphose into a completely different thing. Therefore, in the following studies, the brain tissue slices, which are exposed to air for 10 minutes, are used as the wet tissue slices for the experiment, which likely have optical properties closer to the fresh brain tissues due to the color and the attenuation coefficient of the brain tissues.

Due to the change of the properties of the samples used in this part, another group of new samples was used to for more reasonable and accurate results of the experiment.

B. Simulation setup in Tracepro

An optical model similar to the testing setup in Fig. 3 (b) was built in Tracepro to analyze the light attenuation through

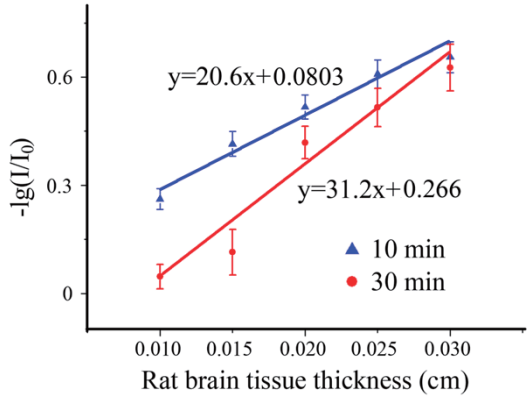

Fig. 4 Attenuation coefficient of LED light through brain tissue slices after exposed in air at room temperature for different time durations.

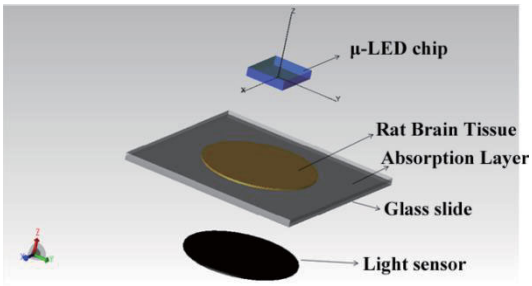

Fig. 5. TracePro model for device simulation.

different thin film samples, in comparison with the experimental data. As shown in Fig. 5, the μ-LED chip used in the simulation had a size of 220 μm × 270 μm × 50 μm with randomly emitted light. Rat brain tissue slice was set as a cylinder with a radius of 500 μm and the height ranging from 100-300 μm for representing different thicknesses. For the simulation of Parylene-C as the inserted object, its thickness was modified to have a range of 15-100 μm to match with the real size of the Parylene-C films. Absorption layer and glass slide both had the size of 1000 μm ×1000 μm ×10 μm. An absorption layer was placed around the sample to absorb the unconsidered light beam while allowing the wanted light going through the sample. The light sensor was set as a cylinder with a radius of 500 μm and a height of 0.5 μm.

C. μ-LED light through rat brain tissue slices

The attenuation coefficients of μ-LED light through the fixed the rat brain tissue slices collected from the experiment and the simulation are shown in Fig. 6. In addition to the LED light source, a laser was used as an alternative light source in the simulation and compared to the LED light source. In the experiment, brain tissue slices with a thickness range of 100-300 μm were measured. Considering the thickness variation of the brain tissue slices due to cutting, three samples were measured for each different thickness of the rat brain tissue slices, and thicknesses of all the tissue slices were measured to ensure the accuracy of the linear fitting. It can be seen that the attenuation coefficient and the thickness of the samples turned out to be linearly dependent. After doing linear fitting with ORIGINPRO, the attenuation coefficient of the fixed brain tissue was calculated to be around 19.9 cm^{-1}, which is lower than the attenuation coefficient of the laser (15 cm^{-1}) reported in [25]. Highly divergent light beams of μ-LED are likely to contribute to this observation. Unlike laser with high directivity, light beams from μ-LED are highly scattered while traveling through the fixed tissue, which leads to a bigger illumination area between the light and the tissue, and eventually, an increased absorption coefficient.

D. μ-LED light through Parylene-C

It is anticipated that the attenuation coefficient of Parylene is much lower than the brain tissue, which is proved by the

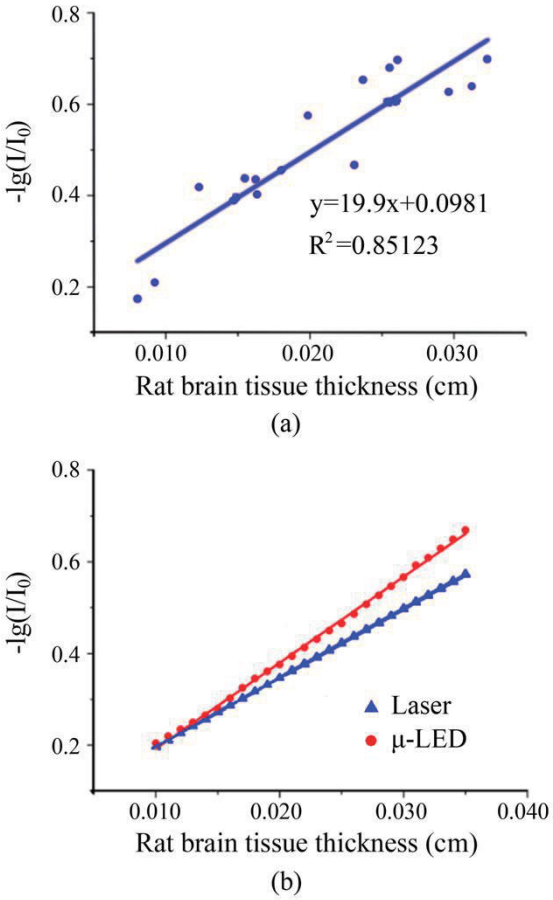

Fig. 6. Attenuation coefficient of μ-LED light through fixed rat brain tissue slices, collected from the experiment (a) and the simulation (b). Simulation was done using both the LED and laser as the light source.

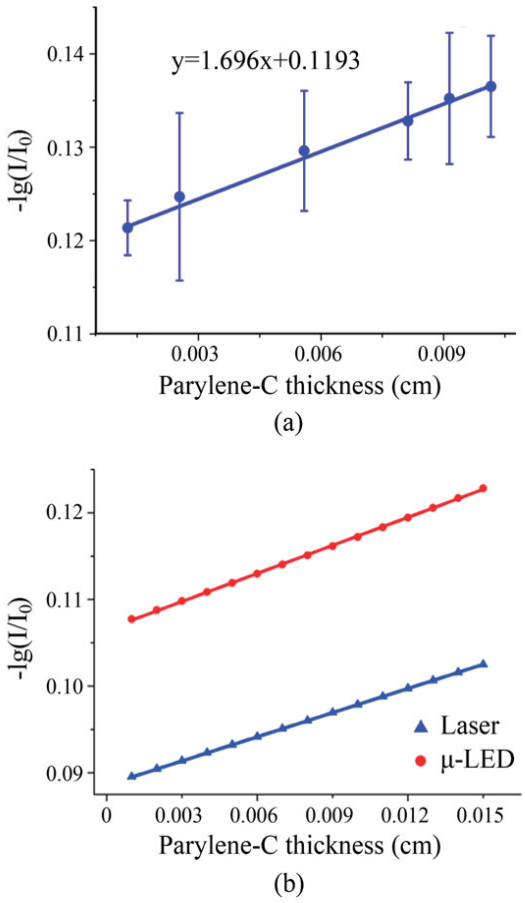

Fig. 7. Attenuation coefficient of μ-LED light through Parylene-C, collected from the experiment (a) and the simulation (b). Simulation was done using both the LED and laser as the light source.

experiment and the simulation, as indicated in Fig. 7. This is most likely to be caused by the inhomogeneous material properties of the brain tissue, which results in more scattering of light. The Parylene samples also exhibited better linearity compared to the brain tissue slices. This may be due to the irregular shape and non-uniform thickness of the tissue slice, which makes light detection inconsistent. Another contribution for this observation may be that the light sensor never senses all the light beams because of the divergence of the μ-LED light beams, as indicated in Fig. 3 (b). While in simulation, there are no such problems existing.

The mismatch between the theoretical and experimental data could be caused by the diverging of μ-LED light beams, which is more prominent in the experiments than in the simulation. In addition, it was noticed that the attenuation coefficient of the laser light source is much lower than that of that of μ-LED, which is mainly attributed to the increased scatter and absorption of the diverge light beams of μ-LED in the samples.

V. Conclusion

In summary we studied the optical propagation of blue LED light in rat's brain tissue and Parylene-C, which could be used to guide the design of the next generation of optogenetic neuromodulators for the brain study. The attenuation coefficients of blue micro-LED light in the rat brain tissue and Parylene-C were measured, which were 19.9 cm^{-1} and 1.70 cm^{-1}, respectively. Experiments are underway to further study the optical propagation of different colors of LED light in the brain tissue to provide more accurate results and data for the comparison with animal experiments.

Acknowledgment

This work was supported by the Electrical, Communications and Cyber Systems Division of the National Science Foundation under Award ECCS-1407880.

References

[1] F. Zhang, et al., "Circuit-breakers: optical technologies for probing neural signals and systems," Nature Reviews Neuroscience, vol. 8, no. 8, pp. 577–581, 2007.

[2] H.S. Mayberg, et al., "Deep brain stimulation for treatment-resistant depression," Neuron, vol. 45, no. 5, pp. 651–660, 2005.

[3] K. Y. Kwon, B. Sirowatka, A. Weber, and W. Li, "Opto-μECoG array: A hybrid neural interface with transparent μECoG electrode array and integrated LEDs for optogenetics," IEEE Trans. Biomed. Circuits Syst., vol. 7, no. 5, pp. 593-600, 2013.

[4] Galvan, A., Hu, X., Smith, Y., and Wichmann, T. (2012). In vivo optogenetic control of striatal and thalamic neurons in non-human primates. PLoS ONE 7, e50808.

[5] Cardin, J.A., Carle´ n, M., Meletis, K., Knoblich, U., Zhang, F., Deisseroth, K., Tsai, L.-H., and Moore, C.I. (2010). Targeted optogenetic stimulation and recording of neurons in vivo using cell-type-specific expression of Channelrhodopsin-2. Nat. Protoc. 5, 247–254.

[6] Jazayeri, M., Lindbloom-Brown, Z., and Horwitz, G.D. (2012). Saccadic eye movements evoked by optogenetic activation of primate V1. Nat. Neurosci. 15, 1368–1370.

[7] Galvan, A., Hu, X., Smith, Y., and Wichmann, T. (2016). Effects of optogenetic activation of corticothalamic terminals in the motor thalamus of awake monkeys. J. Neurosci. 36, 3519–3530.

[8] S. Butovas and C. Schwarz, "Spatiotemporal effects of microstimulation in rat neocortex: A parametric study using multielectrode recordings," J. Neurophsiol., vol. 90, no. 5, pp. 3024-3039, Nov 2003.

[9] Deisseroth, "Optogenetics," Nature Methods 8, 26–29 (2011).

[10] F. Zhang, V. Gradinaru, A. R. Adamantidis, R. Durand, R. D. Airan, L. de Lecea, et al., "Optogenetic interrogation of neural circuits: technology for probing mammalian brain structures," Nat. Protoc., vol. 5, no. 3, pp. 439-456, 2010.

[11] B. Fan, R. Rechenberg, M. F. Becker and W. Li, "Fabrication of polycrystalline diamond on a flexible Parylene substrate," 2015 Transducers - 2015 18th International Conference on Solid-State Sensors, Actuators and Microsystems (TRANSDUCERS), Anchorage, AK, 2015, pp. 892-895.

[12] B. Fan, K. Y. Kwon, A. J. Weber and W. Li, "An implantable, miniaturized SU-8 optical probe for optogenetics-based deep brain stimulation," 2014 36th Annual International Conference of the IEEE Engineering in Medicine and Biology Society, Chicago, IL, 2014, pp. 450-453.

[13] X. Bi, T. Xie, B. Fan, W. Khan, Y. Guo and W. Li, "A Flexible, Micro-Lens-Coupled LED Stimulator for Optical Neuromodulation," in IEEE Transactions on Biomedical Circuits and Systems, vol. 10, no. 5, pp. 972-978, Oct. 2016.

[14] N. McAlinden, D. Massoubre, E. Richardson, E. Gu, S. Sakata, M. D. Dawson, et al., "Thermal and optical characterization of micro-LED probes for in vivo optogenetic neural stimulation," Opt. Lett., vol. 38, no. 6, pp. 992-994, Mar. 2013.

[15] C. T. Wentz, et al., "A wirelessly powered and controlled device for optical neural control of freely-behaving animals," J. Neural Eng., vol. 8, no. 4, p. 10, Aug 2011.

[16] X. Bi, B. Fan, and W. Li, "Micro-lens-coupled LED neural stimulator for optogenetics," in IEEE Int. Conf. on Biomedical Circuits and Systems Conf. (BioCAS), Atlanta, GA, Oct. 2015, pp. 1-4.

[17] K. Y. Kwon, A. Khomenko, M. Haq and W. Li, "Integrated slanted microneedle-LED array for optogenetics," 2013 35th Annual International Conference of the IEEE Engineering in Medicine and Biology Society (EMBC), Osaka, 2013, pp. 249-252.

[18] K. Y. Kwon, H. M. Lee, M. Ghovanloo, A. Weber, and W. Li, "A wireless slanted optrode array with integrated micro LEDs for optogenetics," in IEEE 27th Int. Conf. on Micro Electro Mechanical Systems (MEMS), San Francisco, CA, 2014, pp. 813-816.

[19] N. Grossman, V. Poher, M. S. Grubb, G. T. Kennedy, K. Nikolic, B. McGovern, et al., "Multi-site optical excitation using ChR2 and micro-LED array," J. Neural Eng., vol. 7, no. 1, p. 13, Feb. 2010.

[20] B. McGovern, R. B. Palmini, N. Grossman, E. M. Drakakis, V. Poher, M. A. A. Neil, et al., "A New Individually Addressable Micro-LED Array for Photogenetic Neural Stimulation," IEEE Trans. Biomed. Circuits Syst., vol. 4, no. 6, pp. 469-476, Dec. 2010.

[21] [B. Fan et al., "A polycrystalline diamond-based, hybrid neural interfacing probe for optogenetics," 2015 28th IEEE International Conference on Micro Electro Mechanical Systems (MEMS), Estoril, 2015, pp. 616-619.

[22] Al-Juboori, et al., "Light Scattering Properties Vary across Different Regions of the Adult Mouse Brain," PLoS ONE, 8(7). 2013.